archives
of thermodynamics
Vol. **43**(2022), No. 4, 63–83
DOI: 10.24425/ather.2022.144406

Partially transient one-dimensional thermal-flow model of a heat exchanger, upwind numerical solution method and experimental verification

DARIUSZ KARDAŚ[a]
IZABELA WARDACH-ŚWIĘCICKA[a*]
ARTUR GRAJEWSKI[b]

[a] The Szewalski Institute of Fluid Flow Machinery, Polish Academy of Sciences, Fiszera 14, 80-231 Gdańsk, Poland

[b] HEXONIC Sp. z o.o., Warszawska 50, 82-100 Nowy Dwór Gdański, Poland

Abstract Shell and tube heat exchangers are commonly used in a wide range of practical engineering. The key issue in such a system is the heat exchange between the hot and cold working media. An increased cost of production of these devices has forced all manufacturing companies to reduce the total amount of used materials by better optimizing their construction. Numerous studies on the heat exchanger design codes have been carried out, basically focusing on the use of fully time-dependent partial differential equations for mass, momentum, and energy balance. They are very complex and time-consuming, especially when the designers want to have full information in a full 3D system. The paper presents the 1D mathematical model for analysis of the thermal performance of the counter-current heat exchanger comprised of mixed time-dependent and time-independent equations, solved by the upwind numerical solution method, which allows for a reduction in the CPU time for obtaining the proper solution. The comparison of numerical results obtained from an in-house program called Upwind Heat Exchanger Solver written in a Fortran code, with those derived using commercial software package ASPEN, and those obtained experimentally, shows very good agreement in terms of the temperature and pressure distribution predictions. The proposed method for fast designing calculations appears beneficial for other tube shapes and types of heat exchangers.

Keywords: Heat exchanger; Mathematical modelling; One-dimensional; Mixed model; Shell and tube

*Corresponding Author. Email: izabela.wardach@imp.gda.pl

Nomenclature

A	–	area, m^2
C	–	circumference of the wetted area, m
c_p	–	specific heat, J/(kgK)
D	–	pipe diameter, m
d	–	pipe diameter, m
dP	–	pressure drop, kPa
f	–	friction factor,
g	–	gravity acceleration, = 9.81 m/s^2
h	–	specific enthalpy, J/kg
k	–	heat transfer coefficient, $W/(m^2K)$
L	–	length, m
$\dot{m}$	–	mass flow rate, kg/s
Nu	–	Nusselt number
Pr	–	Prandtl number
p	–	pressure, Pa
Q	–	heat, J
$\dot{Q}$	–	heat source, W
Re	–	Reynolds number
T	–	temperature, K
t	–	time, s
V	–	volume, m^3
w	–	fluid velocity, m/s
z	–	spatial coordinate related to the length of the system, m

Greek symbols

α	–	convective heat transfer coefficient, $W/(m^2K)$
β	–	angle position, rad
δ	–	wall thickness, m
ϵ	–	pipe roughness, m
η	–	efficiency
λ	–	thermal conductivity, W/(mK)
μ	–	dynamic viscosity, Pa s
ρ	–	density, kg/m^3
τ_w	–	shear stress, Pa
ξ	–	coefficient depending on the nature of local resistance
φ	–	angle of pipe bending, rad

Subscripts and superscripts

0	–	calculated area
C	–	cold medium
exp	–	experimental
H	–	hot medium
i	–	ith medium
in	–	inlet
out	–	outlet
w	–	wall

Acronyms

1D	–	one-dimensional
1DP	–	one-dimensional code with assumption of cylindrical wall shape
1DW	–	one-dimensional code with assumption of simple wall shape
CFD	–	computational fluid dynamics
LMTD	–	logarithmic mean temperature difference
NTU	–	number of transfer units
RELAP	–	Reactor Excursion and Leak Analysis Program
TRAC	–	Transient Reactor Analysis Code
UHES	–	Upwind Heat Exchanger Solver

1 Introduction

According to Markets and Markets [1] the value of the global heat exchanger market amounts to 15.6 billion USD, and by 2026 it should reach the value of about 19.9 billion USD, which gives a weighted average growth rate of approximately 5% per annum. The largest increases are expected in the chemical, petrochemical, mining and heating, ventilation and air conditioning (HVAC) industries. A slightly lower pace of growth can be expected in food, energy, sewage, paper and other industries. The highest pace of growth is to be expected in the region of Asia and the Pacific, thanks to its rapidly progressing industrialization. Although the war in Ukraine affected the production dynamics and increased uncertainty, it must be said that heat exchangers are a large world market. Shell and tube exchangers account for 27% of the global market of heat exchangers, which is 5.4 billion USD per year. The highest growth dynamics, of 9%, are expected in the market of plate heat exchangers, including sealed, soldered and welded exchangers, which is the result of the rapidly growing heating, ventilation and air conditioning industry. The outlook for growth of shell and tube heat exchangers is slightly lower, but it is estimated at 6% per annum. Shell and tube heat exchangers are an essential part of energetic and chemical installations so their price usually accounts for a large part of the total cost. For this reason, designers focus on solutions with reduced dimensions and reduced weight to make them more competitive. Therefore, the exact calculations of heat transfer in exchangers are of great technical importance as they affect the proper operation of the whole system and have a significant impact on their price.

2 Designing and modelling heat exchangers performance

The most popular calculation methods for shell and tube heat exchangers include the logarithmic mean temperature difference (LMTD) and the number of transfer units (NTU) method. The LMTD method has been around for a long time [2], it can be found in textbooks [3] and is still used as the basic calculation method [4]. It requires not only the cold and the hot inlet fluid temperatures, but also the outlet temperatures. When the latter is unknown, this method requires an iterative procedure. The NTU method is not an iterative one [5,6], it is based on the knowledge of the media mass flows and only the hot and the cold fluid inlet temperatures. In the shell and tube exchanger, the important part of the heat flux flows through the leaks, therefore the Delaware method [7] can be used, which is more labour-intensive but also more precise because it uses correction coefficients. These coefficients refer to the leaks between parts of the exchanger located in the inter-tube space (tubes, baffles, shell). Leaks have a negative impact on the heat transfer process, which is reflected primarily in the heat conductivity coefficient, as well as in the predicted pressure drop. The aforementioned methods are based on global heat and mass balances in the shell and tube type exchanger, hence they are relatively inaccurate, especially when the flux and heat transfer parameters change. A completely different approach is to use CFD programs, which can take into account the full geometry of an exchanger and three-dimensional flow structures [8,9]. However, computational fluid dynamics (CFD) simulation still requires a lot of work, large computing power, and computing time to create meshes. Therefore, CFD is rarely used to solve practical heat transfer problems.

An alternative to the lumped methods LMTD and NTU on the one hand, and CFD on the other, might be methods based on one-dimensional equations describing the mass, momentum, and energy flows in the hot and cold fluid. Generally, a one-dimensional system of balance equations is used in various fields of science and technology, including pipelines, turbines, compressors, and rocket engines. The methods of modelling non-stationary compressible one-dimensional flows are a scientific research problem in the field of numerical methods in which the main goal is to obtain stable and accurate solutions [10,11]. One area, in which one-dimensional models are particularly attractive, is the two-phase flows, especially when they are applied to nuclear reactors. A number of works are derived from models initiated in the RELAP (Reactor Excursion and Leak Analysis Program) [12]

and TRAC (Transient Reactor Analysis Code) [13] codes, which also have their computational algorithms for solving non-linear systems of difference equations. The one-dimensional approach was developed for models with a non-equilibrium thermodynamic state developed by Bilicki *et al.* [14]. Modern works of Daude *et al.* [15,16] and Delchini *et al.* [17] on two-phase flows also use one-dimensional systems of balance equations and are devoted to developing a method for simulating non-stationary flows in variable geometry pipes. In the work of Chen *et al.* [18], the basic system of equations was transformed into a new form to obtain a coupling matrix equation. As a result, instead of a multi-step solution process, a one-step solution was obtained. Due to the nonlinearity of this type of equations system, the methods of solving them were also analyzed. Such an example is the work by Lopez *et al.* [19], in which a numerical solution based on shifted nodes of the grid was proposed. In this method, the non-stationary terms are approximated by an explicit scheme, which is connected with a partially implicit pressure equation. Difference methods for solving non-stationary systems of equations give good results, but their big disadvantage is the long computational time. This is mainly due to the numerical stability, which must satisfy the Courant–Friedrichs–Lewy condition that depends on the specific difference scheme. In general, however, the time step has to be small to maintain numerical stability, which leads to time-consuming calculations [20].

In the literature, various kinds of one-dimensional models of flows and heat exchange can be found. Roetzel and Das [21] introduced the concept of hyperbolic heat dispersion in fluid. In this approach, the key is the energy equation complemented by the non-equilibrium hyperbolic equation for the heat flux. As a result, partial differential equations are obtained, which are then solved by the Laplace transformation method. A one-dimensional approach was also applied by Luo *et al.* [22] who simulated the dynamics of heat exchangers and studied the responses to changes in the temperature and sudden changes in flow rate. The used model was based on the energy equations for both fluids. An extension of this methodology can be found in the work of Roetzel and Ranong [23], who took into account the variability of the heat transfer coefficient. Yen and Jenkins [24] developed a method to calculate temperature distribution and heat transfer in the exchanger with phase transition, based on one-dimensional energy equations assuming that the convective heat transfer coefficient on each side of the exchanger and the thermal properties of the fluid on the wall are constant. As a result, the fluid and the wall temperature distributions variable in time

and space were obtained. In the paper by Malinowski and Bielski [25] non-stationary temperature distribution in a counter-current heat exchanger was predicted using one-dimensional and non-stationary balance equations with appropriate boundary conditions. The solution method was based on the application of the Laplace transform to a system of partial differential equations, from which a set of ordinary differential equations was obtained and solved analytically. Ansari and Mortazavi [26] showed the dynamic response of a counter-current heat exchanger to inlet parameter changes. The model used for this purpose was based on one-dimensional equations of mass, momentum, and energy balance. This work applies a method that uses the analytical solution of the energy equation. Also, in the work of Yin and Jensen [24], a one-dimensional and non-stationary model of flow and heat transfer in a heat exchanger was used. The subject of the analysis was an influence of an abrupt boundary temperature change on the temperature distribution in the exchanger. The work presents a numerical solution to the problem and its analytical form.

In this paper, a mathematical model for the flow and heat transfer processes in a counter-current shell and tube exchanger under stationary conditions is proposed. The developed computation method is based on a mix of non-stationary and stationary equations for predicting the behaviour of working fluids. The purpose of using this approach is to obtain solutions that take into account changes in thermodynamic parameters along the flow direction. The use of a mixed stationary/non-stationary system of equations to solve a stationary problem is aimed at eliminating iterative methods that may be weakly convergent. The second reason for using such a method is to reduce the computation time.

3 Governing equations

A whole shell-and-tube type heat exchanger may be treated as a tube in a tube system. A schematic of the tested type of heat exchanger is presented in Fig. 1. The thermal-flow model proposed here relates to the calculation of a heat exchanger under steady-state conditions but is based on non-stationary energy balance equations for both hot and cold fluids. The equations of conservation of mass and momentum are stationary.

A partially non-stationary model is designed to simplify and speed up the calculations because the operating conditions are stationary by definition. One-dimensional balance equations for the internal and external fluid

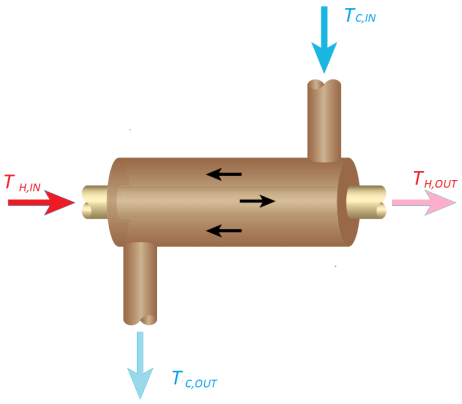

Figure 1: Scheme of a counter-current shell and tube heat exchanger.

provide further simplifications of the model and calculations. Such an approach to geometry and flow significantly reduces the form of differential balance equations and finally, numerical difference equations. The simpler form of balance equations is to reduce the time of numerical computations, which are usually time-consuming. Only horizontal direction is taken into consideration along the pipe length. The model presented here will be applied to single-phase flows, however, it is also suitable for two-phase flows. In the two-phase case, a slightly different way of solving the systems of balance equations should be applied. The physical quantities are assumed to change only with temperature. Details on the derivation of the differential form of the balance equations are given for example in [27].

According to the above assumptions, the thermal-flow model of the heat exchanger consists of the following system of balance equations:

mass balance equation

$$\frac{1}{A_i}\frac{\partial}{\partial z}\left(\rho_i w_i A_i\right) = 0, \tag{1}$$

momentum balance equation

$$\frac{1}{A_i}\frac{\partial}{\partial z}\left(\rho_i w_i w_i A_i\right) + \frac{\partial p_i}{\partial z} = -\tau_{w,i}\frac{C_i}{A_i} + \rho_i g\cos\beta_i\,, \tag{2}$$

energy balance equation

$$\frac{\partial}{\partial t}\left(\rho_i c_{p,i} T_i\right) + \frac{1}{A_i}\frac{\partial}{\partial z}\left(\rho_i w_i c_{p,i} T_i A_i\right) = \frac{\dot{Q}_i}{V_i}\,. \tag{3}$$

The subscript i in Eqs. (1)–(3) denotes the working medium, i.e., for the hot medium $i \equiv H$, for the cold medium $i \equiv C$. Overall, six balance equations should be considered: three for the hot medium and three for the coolant. The densities and the specific heats of individual media are the functions of temperatures, i.e. $\rho_H = \rho_H(T)$, $c_{p,H} = c_{p,H}(T)$, $\rho_C = \rho_C(T)$, $c_{p,C} = c_{p,C}(T)$, for the hot and cold medium, respectively. The quantity $\dot{Q}_i$ (Eq. (3)) represents the source term for heating/cooling. Usually, p stands for the pressure, w is the velocity, A is the surface occupied by the fluid, and C is the circumference of the wetted area.

It shall be noted that in the system, there is no assumption of the thermodynamic equilibrium state between the working media. The term on the right side of Eq. (3) describes the heat transferred from the hot to cold side (if it is written for the hot fluid) or heat absorbed by the cold fluid.

3.1 Source terms

Pressure losses due to the fiction are calculated as follows:

$$\tau_{w,i} = f_i' \frac{\rho_i w_i^2}{2}, \tag{4}$$

where f_i' is the Fanning friction factor coefficient being a function of the Darcy–Weisbach friction factor f depending on the pipe flow regime, i.e. for laminar flow

$$f = \frac{64}{\mathrm{Re}} \quad \text{for} \quad \mathrm{Re} < 2300, \tag{5}$$

for transitional flow

$$f = A_f \mathrm{Re} + B_f \quad \text{for} \quad 2300 < \mathrm{Re} < 4000, \tag{6}$$

and for turbulent flow (Altshul correlation [28])

$$f = 0.11 \left(\frac{\epsilon}{D} + \frac{68}{\mathrm{Re}} \right)^{0.25} \quad \text{for} \quad \mathrm{Re} > 4000. \tag{7}$$

The parameter ϵ is the pipe roughness, D is its diameter, and Re is the Reynolds number. Coefficients A_f and B_f are calculated to fit smoothly curves for the laminar and turbulent regions. Also, the local pressure loss is taken into account [29]:

$$\Delta p_i = \xi \left(\frac{\rho_i w_i^2}{2} \right), \tag{8}$$

where ξ is a coefficient depending on the nature of local resistance. In the case of a hot medium, local pressure losses are associated with the change of the flow cross-section, i.e. flow from/into the bigger/smaller pipe. For the cold medium, they are related to the tube bending by a given angle. The formulas for the ξ values are presented in Table 1.

Table 1: Coefficient ξ for local pressure losses in the analyzed heat exchanger [29].

Case	ξ
From bigger to smaller pipe*	$0.7\left(1-d^2/D^2\right)-0.2\left(1-d^2/D^2\right)^3$
From smaller to bigger pipe*	$\left(1-d^2/D^2\right)^2$
Bending of the pipe for angle*	$0.946\sin(\varphi/2)^2+2.05\sin(\varphi/2)^4$

* D, d – diameters of bigger and smaller pipe, φ – angle of the bending.

The source term in Eq. (3) is defined by

$$Q_i = kA_i\Delta T, \tag{9}$$

where k is the overall heat transfer coefficient, A is the heat transfer surface, and ΔT is the temperature difference between the working fluids. Generally, the heat transferred from the hot side to the cold side is equal to that absorbed by the cold one

$$Q_C = kA_C\left(T_H - T_C\right) = -Q_C. \tag{10}$$

For a simple wall, the overall heat transfer coefficient can be calculated as

$$\frac{1}{k} = \frac{1}{\alpha_H} + \frac{\delta}{\lambda} + \frac{1}{\alpha_C}\,, \tag{11}$$

where δ is the wall thickness, λ is the thermal conductivity of the wall material, and αC and α_H are the convective heat transfer coefficients for cold and hot medium, respectively. For cylindrical walls, the overall heat transfer coefficient can be expressed as

$$\frac{1}{k} = \frac{1}{\alpha_H\dfrac{A_H}{A_0}} + \frac{1}{\dfrac{\lambda}{\delta}\dfrac{d_\mathrm{w}}{d_0}} + \frac{1}{\alpha_C\dfrac{A_C}{A_0}}\,, \tag{12}$$

where d_w is the logarithmic average diameter of the cylindrical wall

$$d_\mathrm{w} = \frac{D_\mathrm{out} - D_\mathrm{in}}{\ln\dfrac{D_\mathrm{out}}{D_\mathrm{in}}}\,. \tag{13}$$

Parameters A_H, A_C are the surfaces calculated from the hot-fluid and cold-fluid side, and A_0 is the calculated area, which depends on the convective heat transfer coefficient as follows:

$$A_0 = A_H \quad \text{for} \quad \alpha_H < \alpha_C \,, \tag{14}$$

$$A_0 = A_C \quad \text{for} \quad \alpha_C < \alpha_H \,. \tag{15}$$

The convective heat transfer coefficient α can be determined from the definition of the Nusselt number:

$$\mathrm{Nu} = \frac{\alpha D}{\lambda} \,. \tag{16}$$

Due to the fact that the correlations connecting Nusselt, Reynolds and Prandtl numbers for the convective heat transfer in pipes are well known, the convective heat transfer coefficient can be easily calculated as a function of flow parameters and geometry. Determination of the Nu number can be obtained from the correlations for laminar and turbulent flows given, respectively, by [29]:

$$\mathrm{Nu} = 3.66 + \frac{0.065 \mathrm{Re}\,\mathrm{Pr}\dfrac{D}{L}}{1 + 0.04\left(\mathrm{Re}\,\mathrm{Pr}\dfrac{D}{L}\right)^{2/3}} \quad \text{for} \quad \mathrm{Re} < 2100, \tag{17}$$

$$\mathrm{Nu} = 0.027 \mathrm{Re}^{0.8} \mathrm{Pr}^{1/3} \left[\frac{\mu(p,T)}{\mu(p,T_\mathrm{w})}\right]^{0.14} \quad \text{for} \quad \mathrm{Re} \geq 2100, \tag{18}$$

where $\mu(p,T)$ is the dynamic viscosity and $\mu(p,T_\mathrm{w})$ is the dynamic viscosity calculated for the wall temperature T_w.

The above partially non-stationary, one-dimensional heat exchanger model consisting of six ordinary and partial differential equations, as well as constitutive and closure equations (Eqs. (1)–(18)), is solved by the method of successive iterations in time. The simplification of the thermal-flow description to two non-stationary energy equations allows for the unambiguous determination of the hot and cold fluid temperature field along the heat exchanger and means that the calculations in time concern only the energy equations. The derivative of temperature over time is approximated by the time finite difference, and the convection term is approximated by the upwind finite difference formula. This numerical scheme allows for explicit calculation of the cold and hot fluid temperatures starting with the

inlet and ending with the outlet. At each time step, both fluid velocities are calculated from the mass balance equation. Knowing the temperature and the velocities at new time steps the pressure distribution can be calculated through the equation of momentum balance, using the same procedure as for the velocity of the fluid. The pressure distribution is determined first for the hot medium (from inlet to outlet) and after that, for the cold medium in the opposite direction. The length of the time step is limited and is dependent on the numerical scheme and space step. The length of both steps is influenced by the stability of the numerical scheme, which can theoretically be determined from the Courant–Friedrichs–Lewy condition. Practically, the time step length is chosen to keep the solution numerically stable. The above assumptions led to the development of a numerical program in the Fortran language called UHES (Upwind Heat Exchanger Solver).

4 Experimental work

4.1 Measurement setup

The experimental set-up consists of four basic systems, which are: a closed system of the tested liquid, a cooling and hot water system and a measuring system. The stand provides the possibility to read and record the temperatures of the working media at the entrance and exit. Figure 2 presents a schematic representation of the locations of thermocouples installed in the experimental setup. Table 2 involves the description of the measurement points.

Table 2: Description of measurement points installed in the experimental setup.

Cold side		
No. 14	Inlet temperature of cooling water	T_C^{in}
No. 15	Outlet temperature of cooling water	T_C^{out}
Hot side		
No. 12	Inlet temperature of hot water	T_C^{in}
No. 13	Outlet temperature of hot water	T_C^{out}

During the conducted tests, the cooling medium was fed to the exchanger with the use of a water pump connected to a flow meter. The cooling water flowed through the exchanger in the external pipe. The applied solution involves counter-current flow, therefore the hot water flows in the opposite direction in the inner pipe.

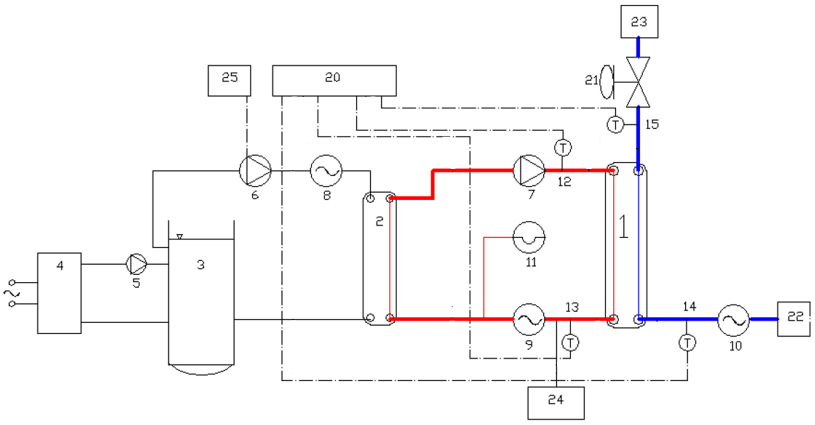

Figure 2: Location of the temperature measurement points installed in the countercurrent heat exchanger experimental setup: 1 – tested system; *2* – indirect heat exchanger; *3* – hot water tank; *4* – heating section; *5–7* – circulation pumps; *8–10* – flow meters; *11* – expansion vessel; *12–15* – temperature sensors; *20* – output for inlet temperature and pressure sensors; *21* – pneumatic regulator valve; *22* – cold water supply; *23* – drain grate; *24* – ultrasonication system; *25* – inverter of the circulation pump.

In order to measure the temperature of water, type Pt100 resistance temperature sensors were used (ranging from -50°C to $+250$°C). All temperature sensors were connected to a multichannel recorder (SIMEX SRT-73).

As aforementioned, the tube-in-tube system was analyzed. The outer diameter of the hot tube was equal to $d_H = 16$ mm and its thickness was 0.8 mm, whereas the outer diameter of the shell was equal to $d_C = 26.9$ mm (2 mm thick). The length of the heat exchanger was $L = 500$ mm.

4.2 Experimental results

Table 3 presents the results from the experimental measurements for different mass flow rates of working fluids. Additionally, for comparison and determining the efficiency of the heat exchanger, the heat transferred from the hot and to the cold side was calculated from the formulas, respectively [30]:

$$\dot{Q}_H = \dot{m}_H \left(h_{H,\text{in}} - h_{H,\text{out}}\right), \tag{19}$$

$$\dot{Q}_C = \dot{m}_C \left(h_{C,\text{out}} - h_{C,\text{in}}\right), \tag{20}$$

Table 3: Results of experimental studies.

Case	Hot side					Cold side					η^{exp}
	$\dot{V}_H^{\mathrm{exp}}$	$\dot{m}_H^{\mathrm{exp}}$	$T_{H,\mathrm{in}}^{\mathrm{exp}}$	$T_{H,\mathrm{out}}^{\mathrm{exp}}$	$\dot{Q}_H^{\mathrm{exp}}$	$\dot{V}_C^{\mathrm{exp}}$	$\dot{m}_C^{\mathrm{exp}}$	$T_{C,\mathrm{in}}^{\mathrm{exp}}$	$T_{C,\mathrm{out}}^{\mathrm{exp}}$	$\dot{Q}_C^{\mathrm{exp}}$	
	l/h	kg/h	°C	°C	kW	l/h	kg/h	°C	°C	kW	%
a	684.0	659.0	97.6	90.3	6.0	655.2	654.7	14.4	21.1	4.8	79
b	680.4	655.5	97.6	90.3	6.0	656.0	655.8	14.4	21.1	4.8	79
c	525.6	503.3	97.2	89.1	5.1	502.6	501.9	14.4	21.9	4.1	80
d	525.6	503.3	97.2	89.1	5.1	502.3	501.8	14.4	21.9	4.1	80
e	525.6	503.3	97.2	89.1	5.1	502.4	449.6	14.4	21.9	4.1	80
f	298.8	288.5	96.0	86.4	3.5	301.7	301.3	14.5	23.4	2.9	84
g	302.4	292.0	96.0	86.4	3.5	301.5	300.2	14.5	23.4	2.9	83
h	302.4	292.0	96.0	86.4	3.5	301.3	300.7	14.5	23.4	2.9	84

where $\dot{m}$ is the mass flow rate and h is the specific enthalpy. The efficiency of the heat exchanger was then obtained from

$$\eta = \frac{\dot{Q}_H}{\dot{Q}_C}\,. \tag{21}$$

For experiments, three mass flow rates were taken into account, the same for both the hot and cold fluids. The tests for each mass flow case were repeated at least twice to be sure that the obtained results are proper. In summarizing, 8 cases were taken into account to determine the efficiency of the stand (cases a–h). It is obvious that the thermal output of the heat exchanger depends on the flow rates of fluids. In the test stand, the maximum obtained thermal duty was at the level of 5 kW and the minimum was about 3 kW for flows around 650 kg/h and 300 kg/h, respectively. As a result, the derived heat exchange effectiveness is at the level of 80% on average and it grows with decreasing flow rates of the media. At each stage of the experiment, efforts were made to maintain the same level of the medium inlet temperatures.

5 Numerical results

The proposed mathematical formulas were implemented in the Fortran numerical code into the program UHES. The results obtained from UHES calculations for the considered test cases are summarized in Tables 1–6.

In Table 4 the results from the Aspen Exchanger Design & Rating package [31] are presented. All the inlet temperatures and the mass flow rates were taken directly from the experimental results. The obtained heat duty is at the same level as experimentally-determined, i.e. it varies from 3 kW to 6 kW. The calculated device efficiency is aproximately 90%, so about 10% higher than those from the experimental studies. In addition, the pressure drop (dP) was also determined using the ASPEN package. It ranges from about 0.3 kPa to 1.2 kPa, depending on the flow rate and has a similar value for both media sides for the same mass flow rates. The similar situation takes place in the case of one-dimensional (1D) in-house code calculations (Tables 5 and 6). The same, as in the Aspen cases, pressure drop was obtained, but the efficiency of the device was set at 100%. The thermal output in those cases varies from 2.7 kW to 5.3 kW, depending on the mass flow rate and the assumed wall shape. For the cylindrical wall, the output increased by about 5% in comparison to the simple wall hypothesis.

Table 4: Results of numerical studies obtained using the ASPEN package.

Case	Hot side					Cold side					η^{Aspen}
	$\dot{m}_H$	$T_{H,\text{in}}$	$T_{H,\text{out}}^{\text{Aspen}}$	dP_H^{Aspen}	$\dot{Q}_H^{\text{Aspen}}$	$\dot{m}_C$	$T_{C,\text{in}}$	$T_{C,\text{out}}^{\text{Aspen}}$	dP_C^{Aspen}	$\dot{Q}_C^{\text{Aspen}}$	
	kg/h	°C	°C	kPa	kW	kg/h	°C	°C	kPa	kW	%
a	659.0	97.6	90.0	1.20	6.3	654.7	14.4	22.2	1.18	5.5	88
b	655.5	97.6	90.0	1.19	6.4	655.8	14.4	22.2	1.18	5.6	87
c	503.3	97.2	88.8	0.72	5.3	501.9	14.4	22.8	0.74	4.6	87
d	503.3	97.2	88.8	0.72	5.3	501.8	14.4	22.8	0.74	4.6	87
e	503.3	97.2	88.9	0.72	5.3	449.6	14.4	22.8	0.73	4.6	87
f	288.5	96.0	87.6	0.25	3.0	301.3	14.5	22.5	0.30	2.6	87
g	292.0	96.0	87.7	0.26	3.0	300.2	14.5	22.6	0.30	2.6	87
h	292.0	96.0	87.7	0.26	3.0	300.7	14.5	22.6	0.30	2.6	87

As may be seen, in the case of temperature prediction all of the predicted values are in good agreement with the experimental results (Exp.) – see Table 7. The difference between the calculated and measured temperature values on the hot side varies from 0.4% to 2.5%, and this value is increasing with the decrease of the hot-fluid mass flow rate. The Aspen predictions (Asp.) are better, due to the assumption of the device efficiency (it is on a similar level as the one from the experiments, whereas for the 1D in-house code it has a higher value, i.e. 90% *vs.* 100%). Assuming the cylindrical wall (1DP) instead of a simple one (1DW), this difference is reduced. Due to the

lack of information about the pressure losses the two numerical methods were compared and presented in Table 8. The difference in the predictions of pressure drop along the heat exchanger tube between the Aspen and 1D in-house codes are at the level of 20% in the case of internal (hot) flow, and from 1% to 30% in the case of external (cold) flow, depending on the mass flow rates. The highest level of this difference refers to the lowest mass flow rate. One should be pointed out: as far as the cold side is considered the lowest obtained pressure drop is about 0.3 kPa. Since in this case, the

Table 5: Results of numerical studies derived using the 1D in-house code adopting the simple wall shape (1DW).

Case	Hot side					Cold side					η^{1DW}
	$\dot{m}_H$	$T_{H,\text{in}}$	$T^{1DW}_{H,\text{out}}$	dP^{1DW}_C	$\dot{Q}^{1DW}_H$	$\dot{m}_C$	$T_{C,\text{in}}$	$T^{1DW}_{C,\text{out}}$	dP^{1DW}_C	$\dot{Q}^{1DW}_C$	
	kg/h	°C	°C	kPa	kW	kg/h	°C	°C	kPa	kW	%
a	659.0	97.6	91.6	1.00	5.0	654.7	14.4	21.4	1.20	5.0	100
b	655.5	97.6	91.6	0.99	5.0	655.8	14.4	21.4	1.21	5.0	100
c	503.3	97.2	90.7	0.60	4.1	501.9	14.4	21.9	0.74	4.1	100
d	503.3	97.2	90.7	0.60	4.1	501.8	14.4	21.9	0.74	4.1	100
e	503.3	97.2	90.8	0.60	4.1	449.6	14.4	21.9	0.74	4.1	100
f	288.5	96.0	88.5	0.21	2.7	301.3	14.5	22.8	0.21	2.7	100
g	292.0	96.0	88.5	0.21	2.7	300.2	14.5	22.8	0.21	2.7	100
h	292.0	96.0	88.5	0.21	2.7	300.7	14.5	22.8	0.21	2.7	100

Table 6: Results of numerical studies obtained using the 1D in-house code adopting the cylindrical wall shape (1DP).

Case	Hot side					Cold side					η^{1DP}
	$\dot{m}_H$	$T_{H,\text{in}}$	$T^{1DP}_{H,\text{out}}$	dP^{1DP}_C	$\dot{Q}^{1DP}_H$	$\dot{m}_C$	$T_{C,\text{in}}$	$T^{1DP}_{C,\text{out}}$	dP^{1DP}_C	$\dot{Q}^{1DP}_C$	
	kg/h	°C	°C	kPa	kW	kg/h	°C	°C	kPa	kW	%
a	659.0	97.6	91.2	1.00	5.3	654.7	14.4	21.9	1.20	5.3	100
b	655.5	97.6	91.2	0.99	5.3	655.8	14.4	21.9	1.21	5.3	100
c	503.3	97.2	90.3	0.60	4.4	501.9	14.4	22.4	0.74	4.4	100
d	503.3	97.2	90.3	0.60	4.4	501.8	14.4	22.4	0.74	4.4	100
e	503.3	97.2	90.3	0.60	4.3	449.6	14.4	22.4	0.74	4.3	100
f	288.5	96.0	88.0	0.21	2.9	301.3	14.5	23.3	0.21	2.9	100
g	292.0	96.0	88.1	0.21	2.9	300.2	14.5	23.4	0.21	2.9	100
h	292.0	96.0	88.1	0.21	2.9	300.7	14.5	23.4	0.21	2.9	100

difference between the pressure drop values derived from Aspen and UHES results is 30%, which gives the value of 90 Pa, this is a not big deviation.

Table 7: Comparison of the numerical results with the experimental values – temperatures for simple and cylindrical wall shapes assumed.

Case	Hot side							Cold side						
	T_H^{out}, °C				ΔT, %			T_C^{out}, °C				ΔT, %		
	Exp.	Asp.	1DW	1DP	Asp.	1DW	1DP	Exp.	Asp.	1DW	1DP	Asp.	1DW	1DP
a	90.3	90.0	91.6	91.2	0.4	1.5	1.0	21.1	22.2	21.4	21.9	5.2	1.5	3.6
b	90.3	89.8	91.6	91.2	0.6	1.4	1.0	21.1	22.2	21.4	21.8	5.3	1.4	3.5
c	89.1	88.8	90.7	90.3	0.3	1.8	1.4	21.9	22.8	21.9	22.4	4.0	0.1	2.2
d	89.1	88.8	90.7	90.3	0.3	1.8	1.4	21.9	22.8	21.9	22.4	4.0	0.1	2.2
e	89.1	88.9	90.8	90.3	0.3	1.9	1.4	21.9	22.8	21.9	22.4	4.1	0.1	2.3
f	86.4	87.6	88.5	88.0	1.4	2.4	1.8	23.4	22.5	22.8	23.3	3.7	2.5	0.3
g	86.4	87.7	88.5	88.1	1.5	2.5	1.9	23.4	22.6	22.9	23.4	3.6	2.3	0.1
h	86.4	87.7	88.5	88.1	1.5	2.5	1.9	23.4	22.6	22.9	23.4	3.6	2.4	0.1

Table 8: Pressure drop – comparison of the numerical results obtained from different programs

Case	Hot side					Cold side				
	dP_H^{Aspen}	dP_H^{1DW}	dP_H^{1DP}	Δp^{1DW}	Δp^{1DP}	dP_C^{Aspen}	dP_C^{1DW}	dP_C^{1DP}	Δp^{1DW}	Δp^{1DP}
	kPa	kPa	kPa	%	%	kPa	kPa	kPa	%	%
a	1.20	1.00	1.00	16.7	16.7	1.18	1.21	1.20	2.1	2.0
b	1.19	0.99	0.99	16.7	16.7	1.18	1.21	1.21	2.2	2.0
c	0.72	0.60	0.60	16.9	16.9	0.74	0.74	0.74	0.9	0.8
d	0.72	0.60	0.60	16.9	16.9	0.74	0.74	0.74	0.8	0.7
e	0.72	0.60	0.60	16.9	16.9	0.73	0.74	0.74	0.8	0.7
f	0.25	0.21	0.21	16.9	16.9	0.30	0.21	0.21	28.7	28.4
g	0.26	0.21	0.21	17.0	17.0	0.30	0.21	0.21	28.8	28.6
h	0.26	0.21	0.21	17.0	17.0	0.30	0.21	0.21	28.8	28.5

In Fig. 3 the results of the numerical 1D program solution concerning the distribution of both medium temperatures along the heat exchanger for case d (see Table 3) are presented. As it may be seen, the hot medium is cooled and the cold one is heated, as it is expected. The outlet hot water temperature is about 10°C lower than its inlet temperature. In the case of coolant, the situation is similar, i.e. the temperature difference between

the inlet and outlet is about 10°C. Those differences are almost equal due to the same flow rates of the working fluids for the discussed case d. The numerical results (lines) are in very good agreement with the experimental ones (points).

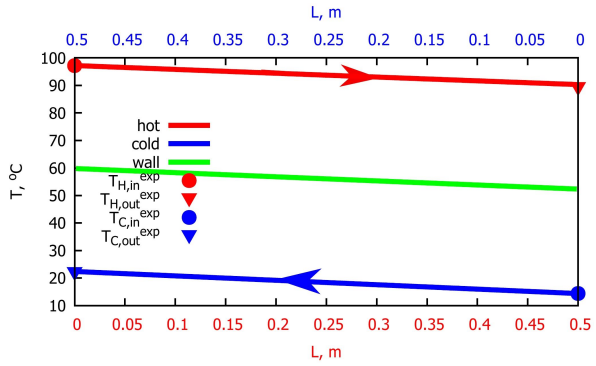

Figure 3: The wall and media temperature distributions along the heat exchanger for case d.

Figures 4–5 illustrate the distribution of the medium temperature in the function of position and time, for hot and cold water, respectively. As it may be noticed, the convergence process takes about 3 s. This is a time for which the assumed convergence limit is achieved. In that time 300 000 iterations with the time step of 10^{-5} s are performed and it results in the CPU real-time of about 40 s. This real-time could be reduced by changing the convergence condition and obtaining the required solution after 50 000 iterations, i.e. in a six times less calculation time (the solution can be achieved after 0.5 s). The temperature of the hot water is decreasing with time and along the tube until it achieves the convergence value, whereas the temperature of the cold water is increasing at the same time (Fig. 5).

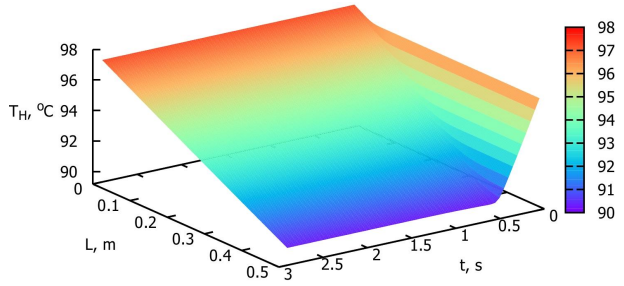

Figure 4: Distribution of the hot medium temperature for case d.

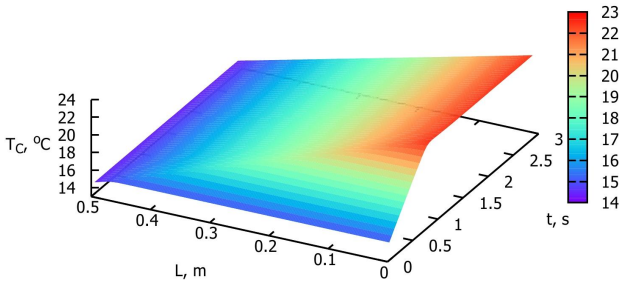

Figure 5: Distribution of the cold medium temperature for case d.

As the present study shows, the proposed 1D mathematical model implemented in a UHES code for the prediction of temperature distribution and pressure losses in the tube heat exchanger is a promising tool for designing simple geometry heat exchangers. The most valuable property of the UHES program is reducing the calculation time. It was shown that it gives values which are in good agreement with the Aspen commercial code results and with our own experimental database.

6 Summary and conclusions

The one-dimensional transient mathematical model was presented and implemented into the in-house Fortran program UHES. The results from the code UHES were experimentally validated based on the authors' own database. The numerical prediction values were in good agreement both with the experimental results of the tested tube-in-tube type heat exchanger and other calculations obtained from the commercial code package Aspen. The analyzed cases yield the thermal output of the exchanger from 3 kW to 5 kW, with the flow rates of working media ranging from 300 kg/h to 650 kg/h, respectively. For the mentioned cases, the difference between the measured and the calculated temperatures does not exceed 2.5%, whereas for the pressure losses this difference was at the level of 20% for the hot side and varies between 1–30% for the cold side, depending on the coolant mass flow rate. The highest percentage difference refers to the laminar flow regime, and the difference between the 1D in-house code results and Aspen code results does not exceed 90 Pa.

The proposed mixed time-dependent and stationary balance equations with the implementation of the upwind finite difference numerical schemes

for the convective terms allows us to obtain a stable and convergent solution. The usage of less-time consuming numerical schemes in UHES leads to the reduction of CPU time and getting the predictions in a very short calculation time. The described in-house code is a promising tool for designing simple geometry heat exchangers. In the future, it can easily be extended for other more complicated geometries including pipes, round-shape and rectangular channels, in which the length is much higher than the characteristic inlet dimension.

Acknowledgment

The work is financed under the program of the Ministry of Education and Science, Implementation Doctorate – 2nd edition, PhD Studies at IMP PAN.

Received 23 September 2022

References

[1] *Heat Exchangers Market by Type (Shell & Tube, Plate & Frame, Air Cooled), Raw Material (Steel, Copper, Aluminum), Application (Chemical, Energy, HVACR, Food & Beverage, Power Generation, Pulp & Paper), and Region – Global Forecast to 2026*. Technical report, Markets and Markets, 2021.

[2] Nagle W.M.: *Mean temperature differences in multipass heat exchangers*. Ind. Eng. Chem. **25**(1933), 6, 604–609.

[3] Serth R.W., Lestina T.G.: *Process Heat Transfer Principles, Applications and Rules of Thumb* (2 Edn.). Academic Press Elsevier, Amsterdam 2014.

[4] Cartaxo S.J.M., Fernandes F.A.N.: *Counter-flow logarithmic mean temperature difference is actually the upper bound: A demonstration*. Appl. Therm. Eng. **31**(2011), 6–7, 1172–1175.

[5] Chen Z., Cheng W., Hu P.: *A new optimization method for heat exchanger design*. Kung Cheng Je Wu Li Hsueh Pao/J. Eng. Thermophys. **34**(2013), 10, 1894–1898.

[6] Vinoth Kumar D., Vijayaraghavan S., Thakur P.: *Analytical and experimental investigation on heat transfer and flow parameters of multichannel louvered fin cross flow heat exchanger using iterative LMTD and ϵ-NTU method*. Mater. Today-Proc. **52**(2022), 1240–1248.

[7] Bell K.J.: *Final Report of the Cooperative Research Program on Shell and Tube Heat Exchangers*. Engineering Experimental Station Bull.: Vol. 5, 1963.

[8] Bartoszewicz J., Bogusławski L.: *Numerical analysis of the steam flow field in shell and tube heat exchanger*. Arch. Thermodyn. **37**(2016), 2, 107–120.

[9] Aziz A., Rehman S.: *Analysis of non-equidistant baffle spacing in a small shell and tube heat exchanger*. Arch. Thermodyn. **41**(2020), 2, 201–221.

[10] Log A.M., Munkejord S.T., Hammer M.: *HLLC-type methods for compressible two-phase flow in ducts with discontinuous area changes*. Comput. Fluids **227**(2021), 105023.

[11] Helluy P., Hérard J., Mathis H.: *A well-balanced approximate Riemann solver for compressible flows in variable cross-section ducts*. J. Comput. Appl. Math. **236**(2012), 7, 1976–1992.

[12] The RELAP5 Development Team: *RELAP5/MOD3 Code Manual: Code Structure, System Models, and Solution Methods*. Prep. for Division of Systems Technology Office of Nuclear Regulatory Research U.S. Nuclear Regulatory Commission, NUREG/CR-5535 INEL-95/0174, Washington D.C. 1995.

[13] Spore J.W., Elson J.S., Jolly-Woodruf S.J., Knight T.D., Lin J.-C., Nelson R.A., Pasamehmetoglu K.Q., Mahaffy J.H., Murray C., Odar F.: *TRACM/ Fortran 90 (Version 3.0) Theory Manual*. Prep. for Division of Systems Technology Office of Nuclear Regulatory Research U.S. Nuclear Regulatory Commission, NUREG/CR-6724, 2001.

[14] Bilicki Z., Kestin J., Pratt M.M.: *A reinterpretation of the results of the moby dick experiments in terms of the nonequilibrium model*. ASME J. Fluids Eng. **112**(1990), 2, 212–217.

[15] Daude F., Galon P.: *Simulations of single- and two-phase shock tubes across abrupt changes of area and branched junctions*. Nucl. Eng. Des. **365**(2020), 110734.

[16] Daude F., Galon P.: *A finite-volume approach for compressible single- and two-phase flows in flexible pipelines with fluid-structure interaction*. J. Comput. Phys. **362**(2018), 375–408.

[17] Delchini M.O., Ragusa J.C., Berry R.A.: *Simulations of single- and two-phase shock tubes and gravity-driven wave problems with the RELAP-7 nuclear reactor system analysis code*. Nucl. Eng. Des. **319**(2017), 106–116.

[18] Chen J., Chen H., Zhang X.: *Implementation and validation of a one-step coupled solution method for the two-fluid model*. Nucl. Eng. Des. **348**(2019), 56–64.

[19] Lopez R., Lecuona A., Nogueira J., Vereda C.: *Numerical solution of one-dimensional transient, two-phase flows with temporal fully implicit high order schemes: Subcooled boiling in pipes*. Nucl. Eng. Des. **313**(2017), 319–329.

[20] Bilicki Z., Kardaś D., Michaelides E.: *Relaxation model for wave phenomena in liquid-vapour bubble flow in channels*. ASME J. Fluids Eng. **120**(1998), 2, 369–377.

[21] Roetzel W., Das S.K.: *Hyperbolic axial dispersion model: concept and its application to a plate heat exchanger*. Int. J. Heat Mass Tran. **38**(1995), 16, 3065–3076.

[22] Luo X., Guan X., Li M., Roetzel W.: *Dynamic behaviour of one-dimensional flow multistream heat exchangers and their networks*. Int. J. Heat Mass Tran. **4**6(2003), 4, 705–715.

[23] Roetzel W., Na Ranong C., Fieg G.: *New axial dispersion model for heat exchanger design*. Heat Mass Transfer **47**(2011), 8, 1009–1017.

[24] Yin J., Jensen M.K.: *Analytic model for transient heat exchanger response*. Int. J. Heat Mass Tran. **46**(2003), 17, 3255–3264.

[25] Malinowski L., Bielski S.: *An analytical method for calculation of transient temperature field in the counter-flow heat exchangers*. Int. Commun. Heat Mass **31**(2004), 5, 683–691.

[26] Ansari M.R., Mortazavi V.: *Simulation of dynamical response of a countercurrent heat exchanger to inlet temperature or mass flow rate change*. Appl. Therm. Eng. **26**(2006), 17–18, 2401–2408.

[27] Puzyrewski R., Sawicki J.: *Basics of Fluids Mechanics and Hydraulics*. PWN, Warszawa 2000 (in Polish).

[28] Genić S., Arandjelović I., Kolendić P., Jarić M., Budimir N., Genić V.: *A review of explicit approximations of Colebrook's equation*. FME Trans. **39**(2011), 2, 67–71.

[29] Hobler T.: *Heat Transfer and Heat Exchangers* (6th Edn.). PWN, Warszawa 1986 (in Polish).

[30] Rup K.: *Calculation of the heat power of a tube heat exchanger*. Arch. Thermodyn. **43**(2022), 1, 127–140.

[31] Aspen Technology, Inc. Aspen Exchanger Design & Rating. https://www.aspentech.com/en/products/engineering/aspen-exchanger-designand-rating (accessed 5 March 2022).